Journal of Taibah University Medical Sciences (2024) 19(1), 164–174

Taibah University

Journal of Taibah University Medical Sciences

www.sciencedirect.com

Original Article

The immunomodulatory activity of *Orthosiphon aristatus* against atopic dermatitis: Evidence-based on network pharmacology and molecular simulations

Thigita A. Pandaleke, M.D. [a,d,*], Kusworini Handono, Ph.D. [b], Dhelya Widasmara, Ph.D. [c] and Hani Susianti, Ph.D. [b]

[a] *Doctoral Program of Medical Science, Universitas Brawijaya, Malang, East Java, Indonesia*
[b] *Department of Clinical Pathology, Faculty of Medicine, Universitas Brawijaya – Saiful Anwar Hospital, Malang, East Java, Indonesia*
[c] *Department of Dermatology and Venereology, Faculty of Medicine, Universitas Brawijaya – Saiful Anwar Hospital, Malang, East Java, Indonesia*
[d] *Department of Dermatology and Venereology, Faculty of Medicine, Sam Ratulangi University, RD Kandou Hospital, Jl. Raya Tanawangko No.56, Manado 95163, North Sulawesi, Indonesia*

Received 15 May 2023; revised 11 August 2023; accepted 26 October 2023; Available online 4 November 2023

الملخص

أهداف البحث: يهدف البحث لاستكشاف النشاط المحتمل لنبات شارب القط السفوي ضد التهاب الجلد التأتبي.

طريقة البحث: تم التعرف على المركبات النباتية من نبات شارب القط السفوي من خلال التحليل الكروماتوجرافي، ثم استمرت الدراسة في تحديد الهدف والشرح الوظيفي لاستكشاف الهدف المحتمل لنبات شارب القط السفوي. بعد ذلك، حددت الدراسة صيدلة الشبكة من البروتينات المشروحة أهداف البروتين للمركبات النباتية لنبات شارب القط السفوي. البروتين ذو المرتبة الأعلى وفقا لخوارزمية البينية والقرب، ثم يستمر في الالتحام الجزيئي ويتم التحقق من صحته من خلال تحليل الديناميكيات الجزيئية.

النتائج: كشف تحليل البيانات الكروماتوغرافية عن ستة وثلاثين مركبا، تصنف في الغالب على أنها حمض الكربوكسيل، والأسيلات الدهنية، والبوليفينول. عند تحديد هذه المركبات، كشف تحديد الهدف القائم على بيولوجيا الشبكة عن نشاطها الحيوي المحتمل في تعديل الالتهاب في التهاب الجلد التأتبي. ظهر عامل نخر الورم ألفا و بروستاغلاندين اتش/جي سينثاز 2 كأهداف محتملة على أساس مركزية المحور في شبكة تفاعل البروتين البروتين. لاحقا، أبرزت تحليلات الالتحام الجزيئي ستة عشر مركبا ذات نشاط مثبط جيد ضد هذين البروتينين. والجدير بالذكر أن محاكاة الديناميكيات الجزيئية كشفت أن ثلاثة مركبات من أصل المركبات الستة عشر المحتملة السابقة كانت أكثر عرضة للعمل كمثبط لعامل نخر الورم ألفا و للبروستاغلاندين اتش/جي سينثاز 2 بالإضافة إلى مثبطها الأصلي. هذه المركبات هي (1آر، 9آر)-5-سيكلوهيكسايل-11-(روبايل سلفونايل)-7، 11-ديازاتريسايكلو[7.3.1.02,7] ترايديكا-2,4-داين-6-1، ويعرف أيضا باسم زينك8297940، كأفضل مثبط لعامل نخر الورم ألفا مع "دي إل-ليوسين أمايد" و بينازول بي كمثبط محتمل للبروستاغلاندين اتش/جي سينثاز 2.

الاستنتاجات: تشير هذه النتائج إلى أن نبات شارب القط السفوي قد يمارس تأثيرات علاجية ضد التهاب الجلد التأتبي عن طريق التحكم في الالتهاب من خلال مسارات إشارات عامل نخر الورم ألفا و بروستاغلاندين اتش/جي سينثاز 2.

الكلمات المفتاحية: التهاب الجلد التأتبي؛ بينازول بي؛ دي إل-ليوسين أمايد؛ مثبط بروستاغلاندين اتش/جي سينثاز 2؛ مثبط عامل نخر الورم ألفا؛ زينك8297940

Abstract

Objectives: To explore the potential activity of *Orthosiphon aristatus* (OA) against atopic dermatitis (AD).

Methods: Phytocompounds from OA were identified through chromatography analysis, then continued to target identification and functional annotation to explore the potential target of OA. Then, network pharmacology from annotated proteins determined protein targets for OA phytocompounds. Protein with highest rank according to the betweenness and closeness algorithm then

* Corresponding address: Doctoral Program of Medical Science, Universitas Brawijaya, Malang, East Java 65145, Indonesia.
E-mail: thagapandaleke@gmail.com (T.A. Pandaleke)

Peer review under responsibility of Taibah University.

Production and hosting by Elsevier

 https://doi.org/10.1016/j.jtumed.2023.10.005

continued to molecular docking and validated through molecular dynamics analysis.

Results: Chromatography data analysis revealed thirty-six compounds, predominantly classified as carboxylic acid, fatty acyls, and polyphenols. Upon identifying these compounds, network biology-based target identification revealed their potential bioactivity in modulating inflammation in AD. Tumour Necrosis Factor-alpha (TNF-α) and Prostaglandin G/H synthase 2 (PTGS2) emerged as the most probable targets based on hub centrality in the protein−protein interaction network. Later, molecular docking analyses highlighted sixteen compounds with good inhibitory activity against these two proteins. Notably, molecular dynamics simulation revealed that three compounds out of the previous sixteen potential compounds were more likely to act as the TNF-α and PTGS2 inhibitor as well as their native inhibitor. Those compounds are (1R,9R)-5-Cyclohexyl-11- (propylsulfonyl)-7,11- diazatricyclo[7.3.1.02,7]trideca- 2,4-dien-6-one, also known as ZINC8297940, as the best TNF-α inhibitor along with dl-Leucineamide and Benazol P as the potential inhibitor of PTGS2.

Conclusions: These findings suggest that OA may exert therapeutic effects against AD by controlling inflammation through TNF-α and PTGS2 signalling pathways.

Keywords: Atopic dermatitis; Benazol P; DL-Leucineamide; PTGS2 inhibitor; TNF-α inhibitor; ZINC8297940

Introduction

Atopic dermatitis (AD) is a chronic inflammatory skin disorder that affects millions of patients on a global scale.[1] AD is characterized by pruritic, erythematous, and eczematous skin lesions and is often associated with a compromised skin barrier function.[2] The pathogenesis of AD is complex and involves various factors, including genetic predisposition, immune dysregulation, and environmental triggers.[3] Amidst these multifaceted causes, certain links between AD and autoimmune factors have emerged.[4–6] Therefore, inflammation appears to be central to the development of AD, and plays a crucial role in initiating and perpetuating the disease process.[7]

Inflammation in AD is mediated by a complex interplay of pro-inflammatory cytokines, chemokines, and immune cells, leading to disruption of the skin barrier, the hyperproliferation of keratinocytes, and the infiltration of immune cells into the skin.[7,8] The standard treatment for AD includes topical corticosteroids, calcineurin inhibitors, and moisturizers, although these treatments may have certain limitations, including potential side effects and preliminary efficacy.[9] Therefore, there is a growing interest in identifying novel therapeutic approaches for AD that can effectively modulate inflammation and promote integrity of the skin barrier.[10] Herbal medicines (HM) stand out among various potential substitutes as a monotherapy or adjuvant therapy for AD.[11] A diverse range of phytocompounds, including alkaloids, flavonoids, terpenes, glycosides, and others, have proved to exert excellent effects in modulating AD, particularly as immunomodulators.[12–14] Hence, investigating naturally occurring phytocompounds may provide good candidates as an alternative or complementary remedy against AD.

Orthosiphon aristatus (OA), commonly known as Java tea or Cat's whiskers, is a traditional medicinal plant that is widely used in Southeast Asia for its anti-inflammatory and antioxidant properties.[15] OA has been reported to possess various pharmacological activities, including anti-inflammatory and anti-oxidative effects.[16] Moreover, OA is also known to exert wound healing activity[17] that helps to recover skin barrier function. Furthermore, clinical studies have also reported the safety of OA as one of the components of Chinese HM.[18] Unfortunately, to our knowledge, there has yet to be a study investigating the potential of OA in modulating inflammation in AD and explaining the underlying mechanism of its bioactivity. Thus, this study aimed to explore the potential activity of OA against AD by regulating immunoactivity.

Materials and Methods

Material

Dried OA leaf powder was obtained from Balai Materia Media, Department of Health, Batu City, East Java, Indonesia (code number: 210826.KKL.F.004). Reagents for compound extraction and phytochemical identification were purchased from Merck.

Extraction of plant compounds

One hundred grams of dried OA leaves were mixed with absolute ethanol (1:10 w/v) and shaken in a rotary shaker for 30 min, followed by overnight maceration. The soluble fraction was then evaporated using a rotary evaporator at 90 °C to remove the solvent. The remaining solvent was evaporated using a heated incubator until a stable weight was obtained. The resulting extract was frozen for future use.

Phytochemical identification

Chromatography procedures for phytochemical screening were performed as described in a previous study using a Thermo Scientific Dionex Ultimate 3000 RSLCnano coupled with a Thermo Scientific Q Exactive Mass Spectrometer.[19] In brief, the extract was dissolved in an aqueous solution prior to injection. The mobile phase consisted of 0.1% formic acid in water as solvent A and 0.1% formic acid in acetonitrile as solvent B, with a Hypersil GOLD aQ 50 mm 1.9 m particle size column as the stationary phase. The chromatography was run for 40 min with a 40 μL/min flow rate. The peaks were then analysed using Compound Discoverer and the mzCloud MS/MS library as the reference database. Compounds with a similarity score of ≥80% were selected for further analysis.

Target identification and biological network construction

Compounds identified by chromatography analysis were entered into SwissTargetPrediction to predict potential protein targets for each compound.[20] Targets with a probability score higher than one were considered as potential targets. Proteins related to atopic dermatitis were also identified in the GeneCard database[21] using keywords such as "atopic dermatitis", "atopic dermatitis inhibitor", and "anti-atopic dermatitis". The proteins obtained from SwissTargetPrediction and the GeneCard database were then analysed using Venny 2.1 to identify overlapping proteins. The overlapping proteins were annotated using the Database for Annotation, Visualization, and Integrated Discovery (DAVID) to analyse biological processes.[22] The biological process with the highest number of targets was selected for protein−protein interaction (PPI) analysis.

The PPI analysis was performed using Cytoscape 3.9.0 with the STRING protein database at a confidence score of 0.8.[23,24] The Cytohubba plugin[25] was used to analyse essential hubs in the constructed protein network. The important hubs were determined based on betweenness and closeness scoring and ranking. The highest-ranking hub for each scoring and ranking function was selected as the target for molecular docking and molecular dynamics simulations.

Three-dimensional structure retrievals

The three-dimensional (3D) structure of compounds was obtained from the PubChem database. The 3D structure was built by Avogadro[26] according to OPSIN: Open Parser for Systematic IUPAC nomenclature for compounds not available in the PubChem database. The Compound ID (CID) and SMILES code are tabulated in Supplementary Table 1. The 3D structures of Tumour Necrosis Factor (TNF)-α and Prostaglandin G/H synthase 2 (PTGS2) were retrieved from the RCSB Protein Data Bank (PDB) with PDB identities 2AZ5 and 5IKR, respectively.[27,28]

Molecular docking

Prior to the docking process, the 3D structures of compounds were energy minimized using OpenBabel[29] in the PyRx package.[30] Furthermore, TNF-α and PTGS2 structures were prepared by removing water and native ligand atoms using Discovery Studio 2019. The native ligand was chosen as the control molecule, or native inhibitor for each protein, and the structure was extracted from the PDB structure using PyMOL. The compounds were considered as flexible ligands, while the proteins were considered as rigid receptors[31] during the docking process using AutoDock Vina 1.2.3 with eight exhaustiveness in the PyRx interface.[32] The grid setting is described in Supplementary Table 2. Compounds with a binding energy of $\leq$7 kcal/mol were selected for protein-ligand analysis by comparing amino acid interactions between the compounds and proteins using Discovery Studio.[33] The 3D structures of protein-ligand complexes were visualized using PyMOL. Protein-ligand complexes exhibiting both interaction similarity to protein-native ligand interactions and a greater number of hydrogen bonds were selected for further molecular dynamics simulations.

Molecular dynamics simulation

YASARA version 21 was used to evaluate structural stability under molecular mechanics simulation.[34] The simulation was run under an AMBER14 forcefield[35] followed by a number of physiological parameters, including a pH of 7.4, an NaCl concentration of 0.9%, a water density of 0.997, a pressure or 1 bar, and a temperature of 310 K.[36] The complex was simulated in a cubic grid shape for a simulation time of 20 ns.

Result and discussion

Phytochemical contents of Orthosiphon leaf extract

Chromatography data analysis revealed thirty-six compounds, predominantly classified as carboxylic acid and fatty acyls, with some carboxylic acids originating from amino acids (Table 1). The compounds with the most significant peak area were Choline and Caffeic Acid, consistent with earlier findings that identified Caffeic Acid and its derivatives as the significant phytochemicals in OA leaves.[37] The presence of Caffeic Acid will enhance OA's anti-inflammatory properties and suppress the AD-like phenotype.[38,39] Moreover, fatty acyl compounds and polyphenols are known to exhibit antioxidant and anti-inflammatory activity for the management of AD.[40] Furthermore, some prenol lipids were identified by chromatography analysis (Table 1). This group of compounds are known to exhibit anti-inflammatory activity by modulating nitric oxide synthase (iNOS) and PTGS2.[15] While most of the compounds identified in this study were not previously reported, they can be developed as anti-inflammatory regulators in addition to those reported previously.

Proteins and biological targets of Orthosiphon leaf extract

SwissTargetPrediction identified approximately 700 potential targets for OA phytocompounds, while the GeneCard database reported over 1000 proteins involved in the pathogenesis of AD. However, only 245 proteins were common to both the SwissTargetPrediction and GeneCard results, thus indicating that these proteins may be the most likely targets for OA (Figure 1A). These findings suggest that these proteins may play a crucial role in the therapeutic effects of OA against AD. Among these proteins, 50 were annotated as being involved in the inflammatory response (as shown in Figure 1B); these proteins are listed in Figure 1C. The identification of 50 proteins involved in the inflammatory response among the standard set of proteins further supports the hypothesis that OA may exert its therapeutic effects in AD by regulating inflammatory events. The inflammatory response has been implicated in the development and progression of AD[41,42]; thus, targeting inflammatory pathways could represent a promising approach for the treatment of AD.[42,43] However, identifying the critical regulatory protein is essential if we are to better modulate inflammatory events in AD.

Network biology or protein−protein interaction (PPI) analysis was conducted to identify the most promising target based on previously identified inflammatory regulatory

Table 1: Phytocompounds identified from the ethanolic extract of *Orthosiphon aristatus*.

Compound No.	Compound name	Formula	Calculated molecular weight	Retention time (min)	Area (Max)
1	Pyrogallol	$C_6H_6O_3$	126.03172	0.827	61,466,799.74
2	4-Acetamidobutanoic acid	$C_6H_{11}NO_3$	145.07369	0.866	63,371,441.24
3	Caprolactam	$C_6H_{11}NO$	113.08413	0.867	40,228,542.43
4	(2S,5aS,8aR)-1-Methyl-6-(4-methylbenzyl)-2-[3-(4-morpholinyl)-3-oxopropyl]octahydropyrrolo[3,2-E][1,4] diazepin-5(2H)-one	$C_{23}H_{34}N_4O_3$	436.24443	0.898	7,969,479.05
5	Isoleucine	$C_6H_{13}NO_2$	131.0945	0.904	161,188,329.71
6	l-Phenylalanine	$C_9H_{11}NO_2$	165.07618	0.931	56,704,526.78
7	Ingenol-3-angelate	$C_{25}H_{34}O_6$	452.21831	0.933	121,277,667.50
8	Thromboxane B2	$C_{20}H_{34}O_6$	408.18953	0.933	102,503,656.38
9	(1R,9R)-5-Cyclohexyl-11- (propylsulfonyl)-7,11-diazatricyclo[7.3.1.02,7]trideca- 2,4-dien-6-one	$C_{20}H_{30}N_2O_3S$	378.19808	0.934	48,100,046.04
10	Choline	$C_5H_{13}NO$	103.09989	0.937	2,447,886,975.37
11	dl-Leucineamide	$C_6H_{14}N_2O$	89.0844	0.94	83,291,610.14
12	d-(+)-Proline	$C_5H_9NO_2$	115.06342	0.94	66,613,509.10
13	Betaine	$C_5H_{11}NO_2$	117.07894	0.94	262,338,080.66
14	6-formyl-10-(hydroxymethyl)-5- methoxy-3-methylidene-2-oxo-2H,3H,3aH,4H,5H,8H,9H,11aHcyclodeca [b]furan-4-yl 2-methylbutanoate	$C_{21}H_{28}O_7$	414.15782	0.943	29,861,968.78
15	(7E,13E)-9,15-dihydroxy-4,10,16-trimethyl-1,5,11-trioxacyclohexadeca-7,13-diene- 2,6,12-trione	$C_{16}H_{22}O_8$	364.10951	0.956	106,265,368.39
16	l-Tyrosine	$C_9H_{11}NO_3$	181.07367	0.958	12,043,022.71
17	[(2R,3S,4S,5R,6R)-3,4,5-trihydroxy- 6-{[(2S,3S,4R,5R)-4-hydroxy-2,5-bis(hydroxymethyl)-3-{[(2E)-3- (3,4,5-trimethoxyphenyl)prop-2- enoyl]oxy} oxolan-2-yl]oxy}oxan-2-yl]methyl 4-hydroxybenzoate	$C_{31}H_{38}O_{17}$	704.1964	0.97	46,376,012.13
18	N-{[(1S,4S,6S)-4-{[5-(2- Fluorophenyl)-1,3,4-oxadiazol-2-yl]methyl}-6-isopropyl-3-methyl-2- cyclohexen-1-yl]methyl} isonicotinamide	$C_{26}H_{29}FN_4O_2$	470.20784	6.74	15,745,373.79
19	Dibenzylamine	$C_{14}H_{15}N$	197.12012	7.432	42,155,207.53
20	Caffeic acid	$C_9H_8O_4$	180.04197	8.174	2,036,691,177.66
21	Diazepam	$C_{16}H_{13}ClN_2O$	284.07674	12.863	33,592,588.02
22	Sulfaphenazole	$C_{15}H_{14}N_4O_2S$	314.08553	12.937	146,744,065.70
23	6-Gingerol	$C_{17}H_{26}O_4$	276.17748	13.07	33,640,454.81
24	Palmitic Acid	$C_{16}H_{32}O_2$	273.27071	14.689	27,822,083.53
25	Shogaol	$C_{17}H_{24}O_3$	276.17748	16.072	10,847,005.17
26	α-Eleostearic acid	$C_{18}H_{30}O_2$	278.22933	17.016	14,425,731.00
27	Benazol P	$C_{13}H_{11}N_3O$	225.09122	18.099	18,037,978.82
28	Dibutyl phthalate	$C_{16}H_{22}O_4$	278.15735	18.117	42,907,860.63
29	12-Oxo phytodienoic acid	$C_{18}H_{28}O_3$	274.19802	18.871	12,857,695.52
30	9(Z),11(E),13(E)-Octadecatrienoic Acid methyl ester	$C_{19}H_{32}O_2$	292.2452	19.462	281,211,957.49
31	17α-Hydroxyprogesterone	$C_{21}H_{30}O_3$	308.2429	19.991	65,742,938.12
32	1,2,3,4-Tetramethyl-1,3- cyclopentadiene	C_9H_{14}	122.10944	20.547	11,496,788.87
33	Ethyl palmitoleate	$C_{18}H_{34}O_2$	282.26058	20.549	51,830,907.75
34	Pinolenic acid	$C_{18}H_{30}O_2$	278.22933	20.558	164,185,936.60
35	4-Methoxycinnamic acid	$C_{10}H_{10}O_3$	178.06271	20.727	19,139,415.22
36	9,11-Dideoxy-9alpha,11alpha-epoxymethanoprostaglandin F2alpha	$C_{21}H_{34}O_4$	310.25861	20.811	168,009,533.13

proteins. However, only 30 proteins were found to form an interconnected PPI network (Figure 2A). Subsequently, the centrality of network topology was analysed based on closeness and betweenness. Nodes with high closeness are typically more central to the network and may act as important hubs of information flow.[44] In the present analysis, TNF-α was identified as the centre point of the network (Figure 2B).

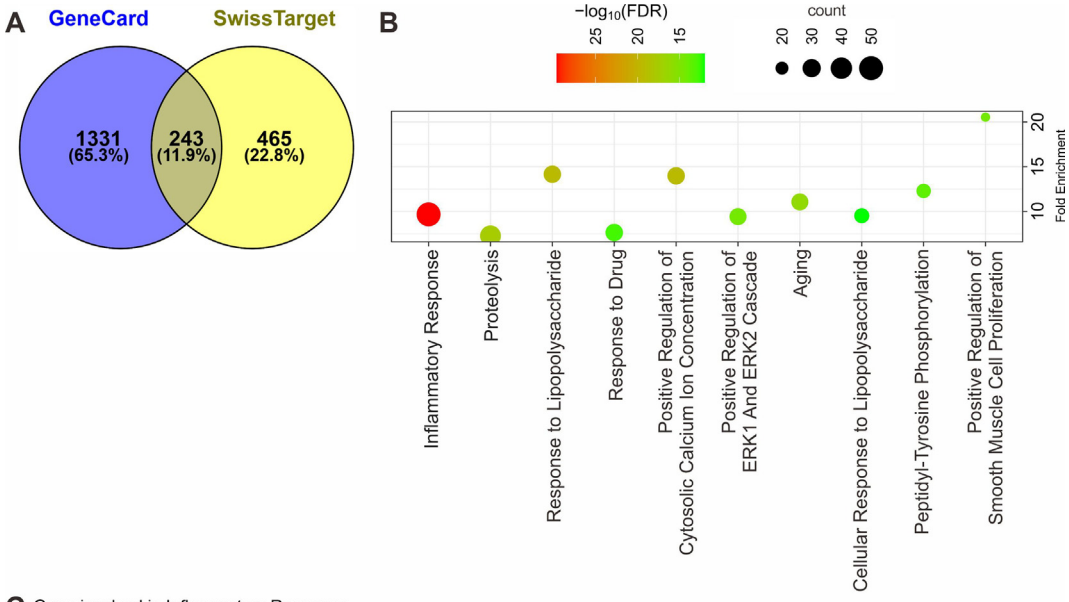

C Gene involved in Inflammatory Response

AKT1	CCR1	CCR2	CCR4	CCR5	CXCR2	HRH1	HRH4	PTGER2
AOC3	ALOX15	BDKRB1	F2R	C5AR1	CHUK	PLA2G2A	PTAFR	PTGER3
KNG1	LTB4R	MIF	MTOR	NOS2	PIK3CD	NFE2L2	FASN	
PTGER4	PTGS1	PTGS2	PRKCQ	RIPK2	STAT3	TLR4	TNF	
NLRP3	RELA	TNFRSF1A	ADORA1	ADORA2A	ADORA3	PTGDR	S1PR3	
TACR1	TBXA2R	IDO1	IKBKB	ITGAL	IL6	PIK3CG	PTGER1	

Figure 1: Target identification of OA phytocompounds through structure–activity relationship analysis using SwissTargetPrediction accompanied by the GeneCard database revealed potential regulatory activity *via* an inflammatory pathway. (A) Venn diagram of the common proteins found as potential targets and proteins involved in the pathogenesis of AD, (B) annotation summary from the common proteins mainly classified as inflammatory regulators, and (C) a list of genes involved in the inflammatory response from previous annotation results.

On the other hand, PTGS2 was ranked highest among all proteins in the network based on betweenness centrality (Figure 2C), thus indicating that this protein can connect between two or more virtual nodes in a particular pathway.[44] A previous study reported that the inhibition of TNF-α and PTGS2 has a beneficial impact on achieving a better prognosis in AD.[45] Furthermore, since cytokines such as TNF-α are known to be crucial for advancing AD, blocking TNF-α will improve the balance to alleviate the AD.[46] This result suggests that TNF-α and PTGS2 are promising targets for the management of AD.

Molecular interaction of the compounds of Orthosiphon with TNF-α and PTGS2

The inhibitory potential of phytocompounds from OA against TNF-α and PTGS2 was investigated using molecular docking to understand the intermolecular chemical interactions involved. Of the compounds identified by chromatography analysis, nine compounds exhibited binding to TNF-α with a binding energy lower than −7.0 kcal/mol, while ten compounds showed similar binding to PTGS2. Compound number 9 and number 18 exhibited lower energy requirements than the native inhibitor of TNF-α (−9.143 and −9.442 against −8.032, respectively), and none of the compounds exhibited a binding energy lower than the native inhibitor of PTGS2 (Table 2 and Supplementary Table 3). Furthermore, most of these compounds interacted with similar residues as the native inhibitors of TNF-α and PTGS2 (Supplementary Table 4). However, only four compounds were selected for further analysis due to their resemblance with the native inhibitor in terms of residue–ligand interaction.

Compounds number 4, number 9, and number 18 showed the most similar interacting residues as the native inhibitor of TNF-α. These compounds also exhibited low binding affinities that were comparable to the native inhibitor. These formed a more significant number of hydrogen bonds compared to other compounds, indicating good stability for inhibitory activity.[47] At least one hydrogen bond, several hydrophobic bonds, and van der Waals interactions, were formed. In contrast, the native inhibitor did not form any hydrogen bonds but formed two halogen bonds between the C and O atoms of GLY121 and the F atom of the native inhibitor (Figure 3). This finding provides preliminary evidence for the inhibitory potential of these three compounds being as good as the native inhibitor.

Similar patterns were observed when considering the PTGS2 complexes. The native inhibitor exhibited the least number of hydrogen bonds when compared to the OA compounds. The native inhibitor formed a carbon–hydrogen bond and several hydrophobic bonds. Three OA compounds, namely compound number 11, number 25, and number 27 exhibited the most similar interacting residues as

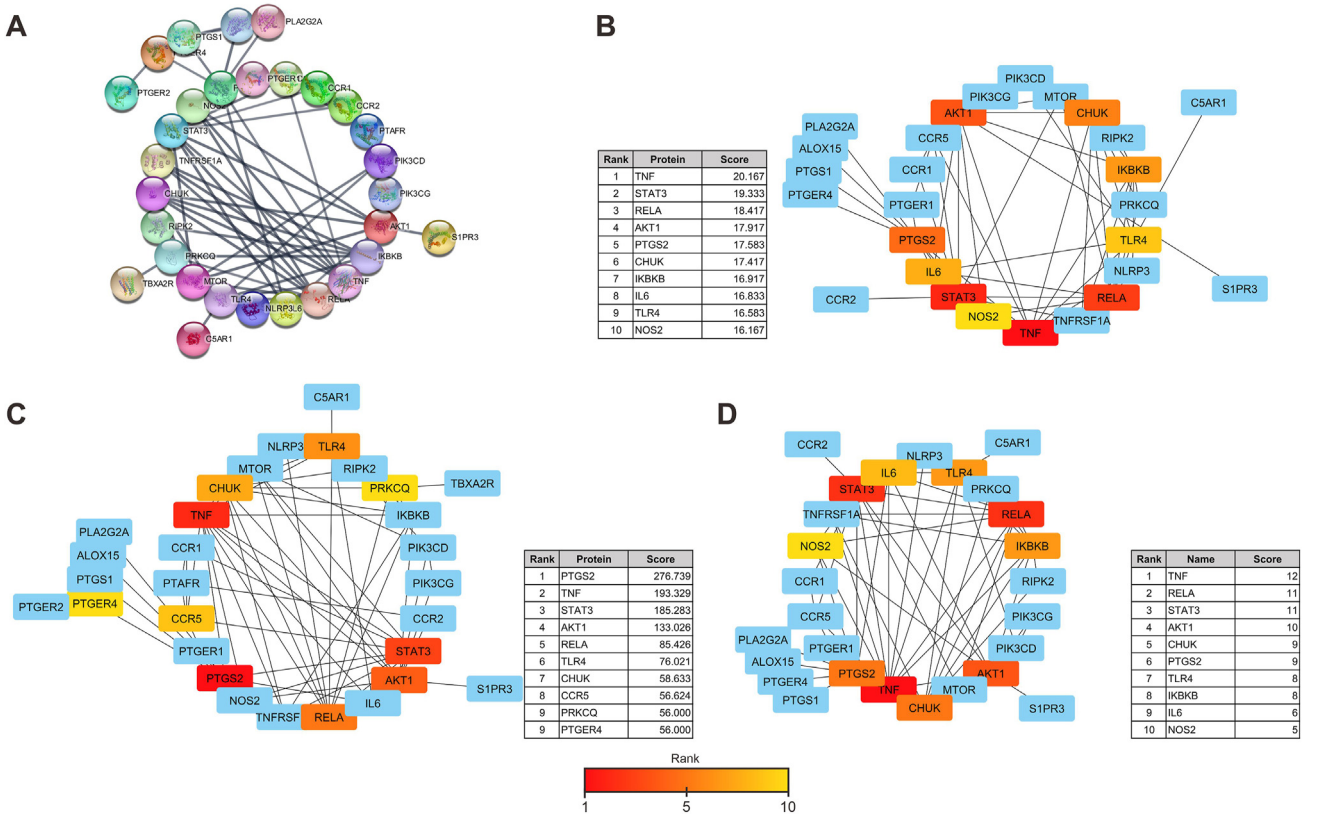

Rank	Protein	Score
1	TNF	20.167
2	STAT3	19.333
3	RELA	18.417
4	AKT1	17.917
5	PTGS2	17.583
6	CHUK	17.417
7	IKBKB	16.917
8	IL6	16.833
9	TLR4	16.583
10	NOS2	16.167

Rank	Protein	Score
1	PTGS2	276.739
2	TNF	193.329
3	STAT3	185.283
4	AKT1	133.026
5	RELA	85.426
6	TLR4	76.021
7	CHUK	58.633
8	CCR5	56.624
9	PRKCQ	56.000
9	PTGER4	56.000

Rank	Name	Score
1	TNF	12
2	RELA	11
3	STAT3	11
4	AKT1	10
5	CHUK	9
6	PTGS2	9
7	TLR4	8
8	IKBKB	8
9	IL6	6
10	NOS2	5

Figure 2: Biological network of the proteins involved in the inflammatory response. (A) Initial network topology of the proteins involved in the inflammatory response, (B) network topology built by the closeness centrality algorithm, (C) network topology of the proteins visualized according to the betweenness centrality algorithm, and (D) the network topology of the proteins visualized according to degree algorithm. The rank and score of the proteins are listed accordingly, followed by different colour intensities of the top ten highest-ranked proteins from each centrality algorithm; the higher the intensity (red), the higher the rank.

Table 2: The calculated binding energy of phytocompounds screened against TNF-α and PTGS2.

TNF		PTGS	
Ligand	Binding Energy (kcal/mol)	Ligand	Binding Energy (kcal/mol)
Inhibitor	−8.432	Inhibitor	−9.391
Compound No. 4	−8.485	Compound No. 11	−8.154
Compound No. 9	−9.143	Compound No. 16	−7.687
Compound No. 7	−8.199	Compound No. 19	−8.342
Compound No. 15	−8.178	Compound No. 22	−7.237
Compound No. 18	−9.442	Compound No. 23	−7.710
Compound No. 21	−7.545	Compound No. 25	−8.209
Compound No. 22	−7.096	Compound No. 26	−7.392
Compound No. 27	−7.626	Compound No. 27	−8.386
Compound No. 31	−8.032	Compound No. 29	−7.496
–		Compound No. 31	−7.201

the native inhibitor. Compound number 11 had the most significant number of hydrogen bonds, while compound number 27 formed an electrostatic bond at ARG120 (Figure 4). As mentioned earlier, these three compounds from OA potentially serve as regulators of PTGS2, in manner similar to the native inhibitor. However, further molecular dynamics simulation is required to understand the structural and binding stability of these compounds when exerting inhibitory activity against their respective receptors. Therefore, these compounds, along with the native inhibitors, will be subjected to molecular dynamics simulation in our future analysis.

Next, the stability of the receptors, ligands, and their binding was assessed by molecular dynamics simulations. This study used several predictors to determine protein structural stability and integrity, including the Root-Mean-Square Deviation (RMSD) of backbone atoms, the Root-Mean-Square Fluctuation (RMSF) of residues, and the Solvent Accessible Surface Area (SASA).[33,36,48] The RMSD of ligand conformation evaluates ligand conformational stability. In contrast, ligand movement and the number of hydrogen bonds were used to assess the binding stability of the ligands to their respective receptors.[33,36]

The molecular dynamics results revealed that the binding of the native inhibitor and selected OA compounds had minimal impact on the stability of TNF-α, as indicated by slight fluctuations in the RMSD of the backbone atoms, RMSF, and SASA (Figure 5A–C). Some residues (GLU25:B, HIS73:B, and ARG103:B) appeared to be less stable, particularly from the TNF-α-native inhibitor complex (Figure 5B). However, minor differences were observed in PTGS2-compound number 11, where SASA

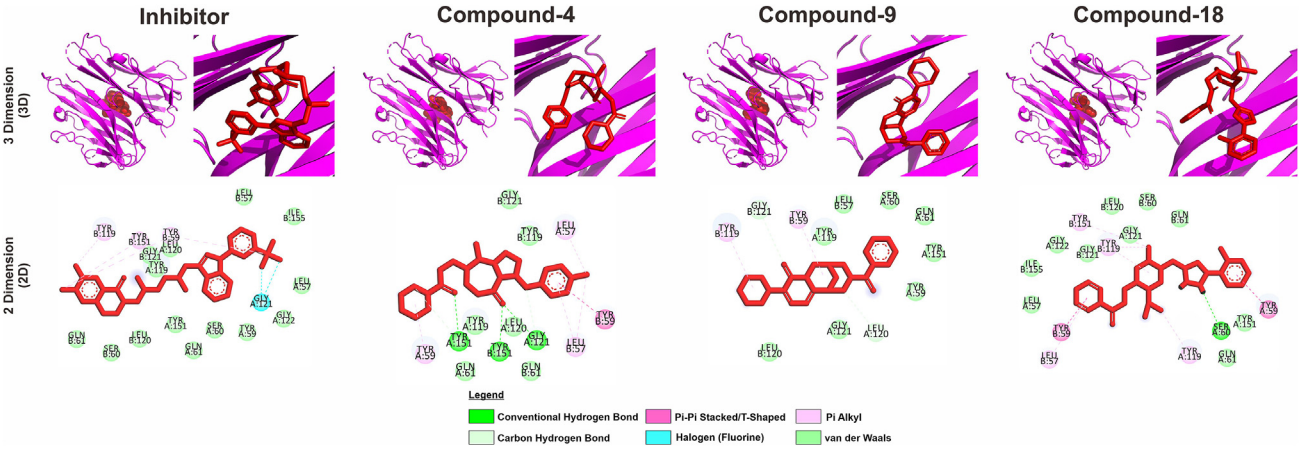

Figure 3: Structural visualization of TNF-α interacting with a native inhibitor and selected OA phytocompounds in both 3D and 2D. In the 3D visualization, the protein is coloured in magenta ribbons, while the structures of the compounds are represented in red spheres or sticks. The 2D interaction scheme describes the interactions between residues and ligands for each complex.

peaked around 10th ns and then dropped towards the end of the simulations (Figure 6C). Nonetheless, the RMSD of backbone atoms and RMSF showed minor differences between native ligands and OA compounds (Figure 6A–B). Less fluctuating residues were exhibited by PTGS2-compound complexes than TNF-α-compound complexes, with LYS83 and TYR134 observed to have RMSF values beyond 4 Å (Figure 6B). Since the stability of the protein structure, particularly in the vicinity of the binding site, can determine the strength and duration of these interactions,[49,50] a stable protein structure can provide a favourable environment for ligand binding and facilitates the formation of stable protein-ligand complexes.[49,50] Accordin-gly, all simulated complexes were able to exhibit robust inhibitory activity during the simulation time, but not with PTGS2-compound number 11.

The conformational stability of a ligand during binding is also crucial. A ligand with a stable conformation can adopt and maintain an optimal binding position, thus allowing for stronger interactions with the protein and increased inhibitory activity.[51] Thus, compound number 9 might may have exhibited the most stable inhibitory activity to TNF-α throughout the simulation time (Figure 5D). Furthermore, all ligands of PTGS2 showed excellent conformational stability to support more decisive inhibitory action (Figure 6D). This event is also associated with the structure of a compound, as most of the selected ligands of TNF-α had more rotatable bonds than the ligands of PTGS2.

Furthermore, the binding stability of the ligands from TNF-α complexes showed variable results, with compound number 9 out-performing the native ligand and other compounds with regards to binding stability, regardless of the number of hydrogen bonds (Figure 5E–F). This data also highlights the importance of conformational stability in terms of the stability of a ligand binding to its receptor.[51]

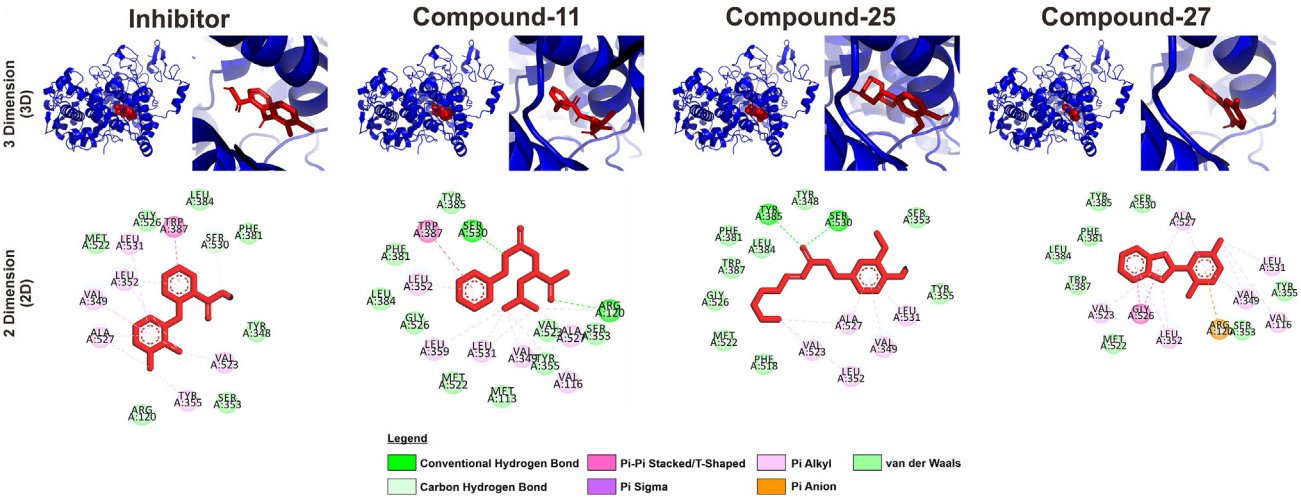

Figure 4: Structural visualization of PTGS2 interacting with a native inhibitor and selected OA phytocompounds in both 3D and 2D. In 3D visualization, the protein is coloured in blue ribbons, while the structure of the compounds is represented by red spheres or sticks. The 2D interaction scheme describes the interactions between residues and ligand atoms for each complex.

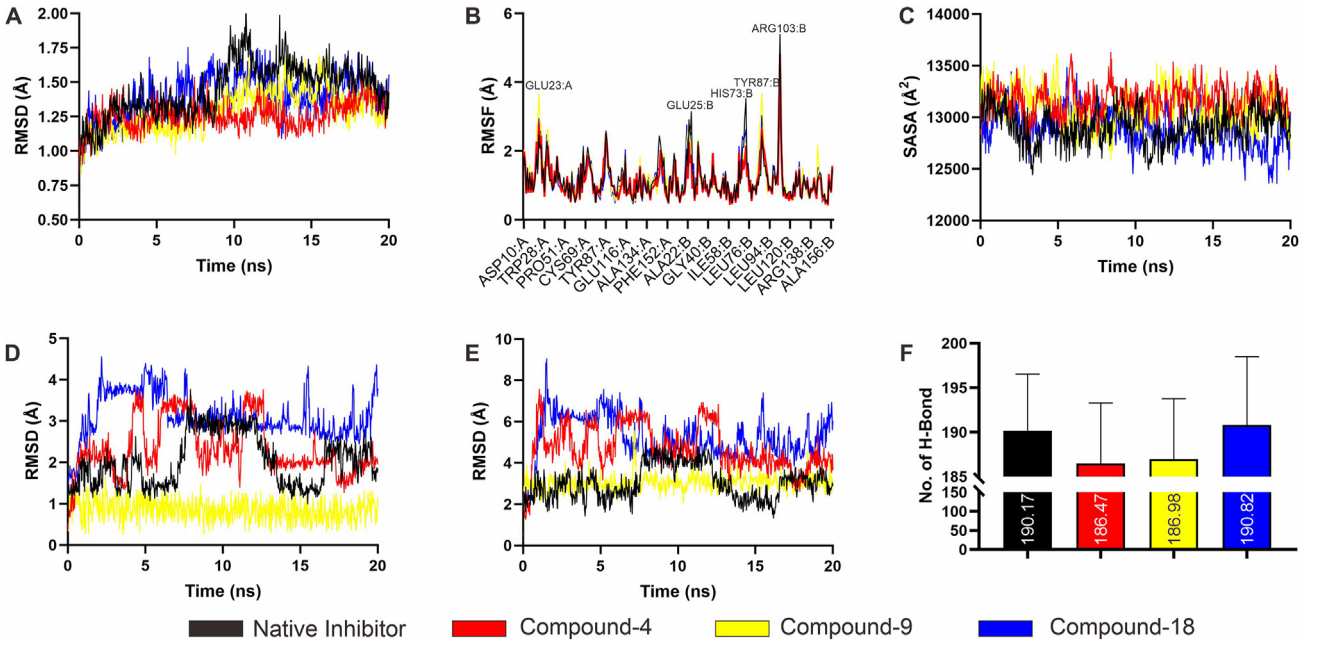

Figure 5: Structural stability evaluation of TNF-α complexes showed that compound number 9 represented a stable inhibitor across different simulation times. (A) RMSD of backbone atoms, (B) RMSF of each residue of TNF-α, (C) SASA, (D) RMSD of ligand conformation, (E) RMSD of ligand movement, and (F) the number of hydrogen bonds in a solute or complex.

On the other hand, almost all of the selected compounds, except for compound number 25, exhibited stable binding stability towards PTGS2. However, there was a logarithmic escalation in the RMSD of ligand movement in compound number 25 from the beginning of the simulations (Figure 6E). Nevertheless, the impact of solute hydrogen bonds on the binding stability among the simulated complexes was indifferent (Figure 6F). Therefore, this study also demonstrates that the importance of hydrogen bonds in ligand binding stability is conditional and depends on the interaction of donors and acceptors of hydrogen bonds with the water as a solvent.[47]

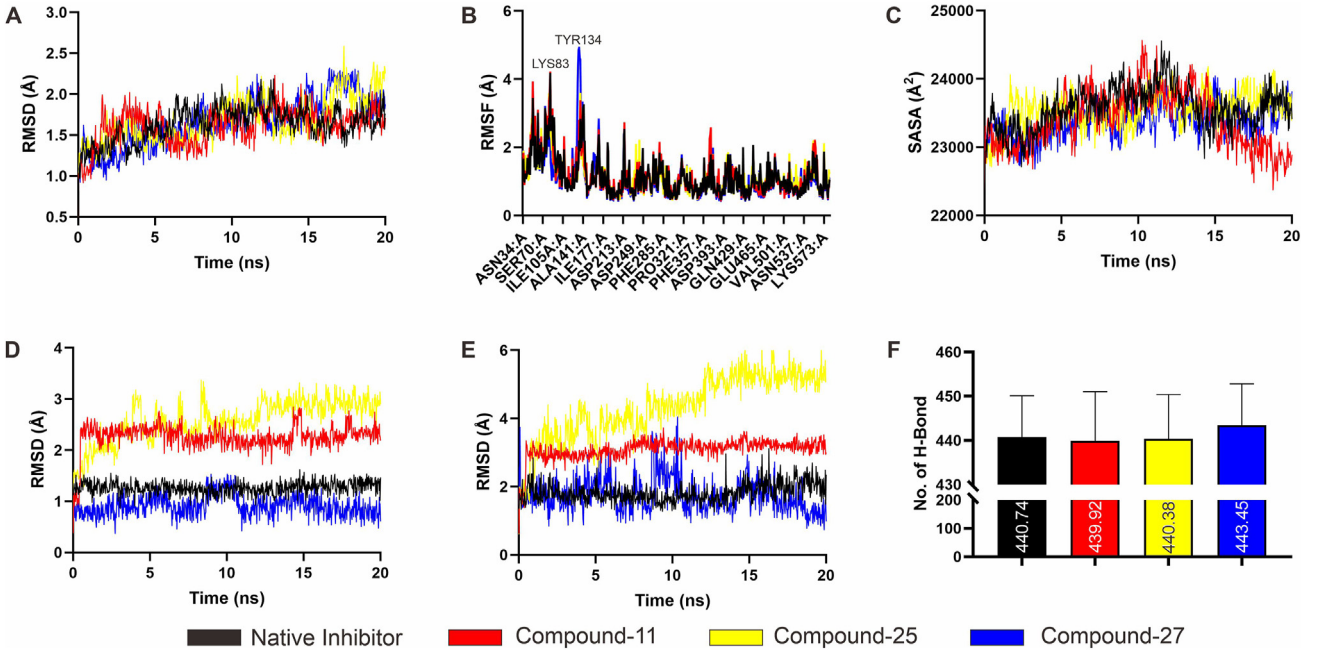

Figure 6: Structural and binding stability evaluation of PTGS2 complexes using molecular dynamics simulation over 20 ns. (A) the RMSD of backbone atoms, (B) the RMSF of each residue of TNF-α, (C) the SASA, (D) the RMSD of ligand conformation, (E) the RMSD of ligand movement, and (F) the number of hydrogen bonds in a solute or complex.

Referring to the simulation results, it is clear that compound number 9 is suspected as the promising TNF inhibitor. With the sole exception of compound number 25, the group of PTGS2 ligands demonstrated favourable inhibitory potential and were distinguished by conformational solid equilibrium and binding consistency. Although there have been few in-depth studies into the specific bioactivity of compound 9, this has been correctly identified as an alkaloid entity. Despite this, the larger family of alkaloid compounds has attracted significant attention for its admirable anti-AD properties.[12,52] On the other hand, compound number 11 (dl-Leucineamide) is a leucine derivative reported to inhibit mTOR signalling.[53] Such targeted inhibition can improve abnormal autoreactive T-cell responses and reduce the inflammatory environment.[54,55] Notably, compound number 27, also known as Benazol P or Drometrizole, is a cosmetic ingredient recognized for its ability to absorb ultraviolet (UV) radiation.[56] Introducing photoprotective attributes augments the therapeutic armamentarium for treating AD and provides a sophisticated approach to improve the efficacy of treatment.[57] In summary, these results highlight the potential of compound number 9 as a TNF-α inhibitor and suggests its promising inhibitory properties for most PTGS2 ligands, while compound number 11 shows potential to inhibit mTOR signalling and the UV-absorbing characteristics of compound number 27 could enhance AD treatments.

Conclusion

Our chromatography analysis predominantly detected carboxylic acids, fatty acyls, and polyphenols as the primary phytoconstituents in the ethanolic extract of OA. Upon identifying these phytocompounds, network biology-based target identification revealed their potential bioactivity for modulating the inflammation of AD. Notably, TNF-α and PTGS2 emerged as the most probable targets based on hub centrality in the protein−protein interaction network. Subsequently, molecular docking analyses highlighted sixteen compounds with good inhibitory activity against TNF-α and PTGS2. However, only six of these compounds exhibited binding site similarities that were comparable to those of native inhibitors for each target. Further analysis, using molecular dynamics simulations, identified compound number 9 as the most promising inhibitor of TNF-α, while compounds 11 and 27 showed the highest potential as PTGS2 inhibitors. Nonetheless, additional studies are now warranted to validate these findings and explore other potential targets for controlling inflammation in AD.

Source of funding

This research received no specific grant from funding agencies in the public, commercial, or not-for-profit sectors.

Conflict of interest

The authors have no conflict of interest to declare.

Ethical approval

This study did not require ethical approval.

Authors contributions

TAP: Conceptualization; Investigation; Writing - original draft. KH: Writing - review & editing; Supervision. DW: Writing - review & editing; Supervision. HS: Writing - review & editing; Supervision. All authors have critically reviewed and approved the final draft and are responsible for the content and similarity index of the manuscript.

Acknowledgement

The authors thank their colleagues in the Doctoral Program of Medical Science, Universitas Brawijaya, for providing constructive comments during the preparation of this manuscript.

Appendix A. Supplementary data

Supplementary data to this article can be found online at https://doi.org/10.1016/j.jtumed.2023.10.005.

References

1. Reynolds M, Gorelick J, Bruno M. Atopic dermatitis: a review of current diagnostic criteria and a proposed update to management. **J Drugs Dermatol 2020**; 19(3): 244−248.
2. Ständer S. Atopic dermatitis. **N Engl J Med 2021**; 384(12): 1136−1143.
3. Chong AC, Visitsunthorn K, Ong PY. Genetic/environmental contributions and immune dysregulation in children with atopic dermatitis. **J Asthma Allergy 2022**; 15: 1681−1700.
4. Wu LC, Hwang CY, Chung PI, Hua TC, Chen YD, Chu SY, et al. Autoimmune disease comorbidities in patients with atopic dermatitis: a nationwide case-control study in Taiwan. **Pediatr Allergy Immunol 2014**; 25(6): 586−592.
5. Lu Z, Zeng N, Cheng Y, Chen Y, Li Y, Lu Q, et al. Atopic dermatitis and risk of autoimmune diseases: a systematic review and meta-analysis. **Allergy Asthma Clin Immunol 2021**; 17(1): 96.
6. Fuxench ZCC, Mitra N, Hoffstad OJ, Phillips EJ, Margolis DJ. Association between atopic dermatitis, autoimmune illnesses, Epstein-Barr virus, and cytomegalovirus. **Arch Dermatol Res 2023**; 315(9): 2689−2692.
7. Skabytska Y, Kaesler S, Volz T, Biedermann T. The role of innate immune signaling in the pathogenesis of atopic dermatitis and consequences for treatments. **Semin Immunopathol 2016**; 38(1): 29−43.
8. Egawa G, Weninger W. Pathogenesis of atopic dermatitis: a short review. In: Ginhoux F, editor. **Cogent Biology**, vol. 1(1); 2015, 1103459.
9. Udkoff J, Waldman A, Ahluwalia J, Borok J, Eichenfield LF. Current and emerging topical therapies for atopic dermatitis. **Clin Dermatol 2017**; 35(4): 375−382.
10. Stevens NE, Cowin AJ, Kopecki Z. Skin barrier and autoimmunity—mechanisms and novel therapeutic approaches for autoimmune blistering diseases of the skin. **Front Immunol 2019**; 10: 1089.

11. Kwon CY, Lee B, Kim S, Lee J, Park M, Kim N. Effectiveness and safety of herbal medicine for atopic dermatitis: an overview of systematic reviews. **Evid Based Complement Alternat Med 2020**; 2020:4140692.
12. Wu S, Pang Y, He Y, Zhang X, Peng L, Guo J, et al. A comprehensive review of natural products against atopic dermatitis: flavonoids, alkaloids, terpenes, glycosides and other compounds. **Biomed Pharmacother 2021**; 140:111741.
13. Ariffin NHM, Hasham R. Potential dermatological application on Asian plants. **Biotechnol Bioproc Eng 2016**; 21(3): 337–354.
14. Lee JH, Jo EH, Lee B, Noh HM, Park S, Lee YM, et al. Soshiho-Tang, a traditional herbal medicine, alleviates atopic dermatitis symptoms via regulation of inflammatory mediators. **Front Pharmacol 2019**; 10: 742.
15. Hsu CL, Hong BH, Yu YS, Yen GC. Antioxidant and anti-inflammatory effects of Orthosiphon aristatus and its bioactive compounds. **J Agric Food Chem 2010**; 58(4): 2150–2156.
16. Hwang JW, Choi JH, Kang SM, Lee SG, Kang H. Antioxidant and anti-inflammatory effects of hot water and ethanol extracts from endemic plants in Indonesia. **Biomed Sci Lett 2021**; 27(3): 161–169.
17. Asraf MH, Sani NS, Williams CD, Jemon K, Malek NANN. In situ biosynthesized silver nanoparticle-incorporated synthesized zeolite A using Orthosiphon aristatus extract for in vitro antibacterial wound healing. **Particuology 2022**; 67: 27–34.
18. Cai X, Sun X, Liu L, Zhou Y, Hong S, Wang J, et al. Efficacy and safety of Chinese herbal medicine for atopic dermatitis: evidence from eight high-quality randomized placebo-controlled trials. **Front Pharmacol 2022**; 13:927304.
19. Purwanti E, Hermanto FE, Prihanta W, Permana TI. Unfolding biomechanism of Dolichos lablab bean as a dietary supplement in type 2 diabetes mellitus management through computational simulation. **Res J Pharm Technol 2022**; 15(7): 3233–3240.
20. Daina A, Michielin O, Zoete V. SwissTargetPrediction: updated data and new features for efficient prediction of protein targets of small molecules. **Nucleic Acids Res 2019**; 47(W1): W357–W364.
21. Safran M, Rosen N, Twik M, BarShir R, Stein TI, Dahary D, et al. The GeneCards Suite. In: Abugessaisa I, Kasukawa T, editors. *Practical guide to life science databases*. Singapore: Springer Nature; 2021. pp. 27–56.
22. Sherman BT, Hao M, Qiu J, Jiao X, Baseler MW, Lane HC, et al. DAVID: a web server for functional enrichment analysis and functional annotation of gene lists (2021 update). **Nucleic Acids Res 2022**; 50(W1): W216–W221.
23. Otasek D, Morris JH, Bouças J, Pico AR, Demchak B. Cytoscape Automation: empowering workflow-based network analysis. **Genome Biol 2019**; 20(1): 185.
24. Szklarczyk D, Gable AL, Nastou KC, Lyon D, Kirsch R, Pyysalo S, et al. The STRING database in 2021: customizable protein–protein networks, and functional characterization of user-uploaded gene/measurement sets. **Nucleic Acids Res 2021**; 49(D1): D605–D612.
25. Chin CH, Chen SH, Wu HH, Ho CW, Ko MT, Lin CY. cytoHubba: identifying hub objects and sub-networks from complex interactome. **BMC Syst Biol 2014**; 8(4): 1–7.
26. Hanwell MD, Curtis DE, Lonie DC, Vandermeersch T, Zurek E, Hutchison GR. Avogadro: an advanced semantic chemical editor, visualization, and analysis platform. **J Cheminf 2012**; 4(1): 17.
27. He MM, Smith AS, Oslob JD, Flanagan WM, Braisted AC, Whitty A, et al. Small-molecule inhibition of TNF-alpha. **Science 2005**; 310(5750): 1022–1025.
28. Orlando BJ, Malkowski MG. Substrate-selective inhibition of cyclooxygeanse-2 by fenamic acid derivatives is dependent on peroxide tone. **J Biol Chem 2016**; 291(29): 15069–15081.
29. O'Boyle NM, Banck M, James CA, Morley C, Vandermeersch T, Hutchison GR. Open Babel: an open chemical toolbox. **J Cheminf 2011**; 3(1): 33.
30. Dallakyan S, Olson AJ. Small-molecule library screening by docking with PyRx. **Methods Mol Biol 2015**; 1263: 243–250.
31. Hermanto FE, Rifa'i M, Widodo. Potential role of glyceollin as anti-metastatic agent through transforming growth factor-β receptors inhibition signaling pathways: a computational study. **AIP Conf Proc 2019**; 2155(1):020035.
32. Eberhardt J, Santos-Martins D, Tillack AF, Forli S. AutoDock Vina 1.2.0: new docking methods, expanded force field, and Python bindings. **J Chem Inf Model 2021**; 61(8): 3891–3898.
33. Hermanto FE, Warsito W, Rifa'i M, Widodo N. On the hypolipidemic activity of elicited soybeans: evidences based on computational analysis. **Indones J Chem 2022**; 22(6): 1626–1636.
34. Krieger E, Vriend G. New ways to boost molecular dynamics simulations. **J Comput Chem 2015**; 36(13): 996–1007.
35. Maier JA, Martinez C, Kasavajhala K, Wickstrom L, Hauser KE, Simmerling C. ff14SB: improving the accuracy of protein side chain and backbone parameters from ff99SB. **J Chem Theory Comput 2015**; 11(8): 3696–3713.
36. Hermanto FE, Warsito W, Rifa'i M, Widodo N. Understanding hypocholesterolemic activity of soy isoflavones: completing the puzzle through computational simulations. **J Biomol Struct Dyn 2023**; 41(19): 9931–9937.
37. Sumaryono W, Proksch P, Wray V, Witte L, Hartmann T. Qualitative and quantitative analysis of the phenolic constituents from Orthosiphon aristatus. **Planta Med 1991**; 57(2): 176–180.
38. Jeon YD, Kee JY, Kim DS, Han YH, Kim SH, Kim SJ, et al. Effects of Ixeris dentata water extract and caffeic acid on allergic inflammation in vivo and in vitro. **BMC Complement Altern Med 2015**; 15(1): 196.
39. Jeong H, Shin JY, Lee K, Lee SJ, Chong HJ, Jeong H, et al. Caffeoyl-prolyl-histidine amide inhibits Fyn and alleviates atopic dermatitis-like phenotypes via suppression of NF-κB activation. **Int J Mol Sci 2020**; 21(19): 7160.
40. Chew YL. The beneficial properties of virgin coconut oil in management of atopic dermatitis. **Pharmacogn Rev 2019**; 13(25): 24–27.
41. Elmariah SB, Lerner EA. The missing link between itch and inflammation in atopic dermatitis. **Cell 2013**; 155(2): 267–269.
42. Tang TS, Bieber T, Williams HC. Are the concepts of induction of remission and treatment of subclinical inflammation in atopic dermatitis clinically useful? **J Allergy Clin Immunol 2014**; 133(6): 1615–1625.e1.
43. Haddad EB, Cyr SL, Arima K, McDonald RA, Levit NA, Nestle FO. Current and emerging strategies to inhibit type 2 inflammation in atopic dermatitis. **Dermatol Ther (Heidelb). 2022**; 12(7): 1501–1533.
44. Gursoy A, Keskin O, Nussinov R. Topological properties of protein interaction networks from a structural perspective. **Biochem Soc Trans 2008**; 36(6): 1398–1403.
45. Park JH, Yeo IJ, Han JH, Suh JW, Lee HP, Hong JT. Anti-inflammatory effect of astaxanthin in phthalic anhydride-induced atopic dermatitis animal model. **Exp Dermatol 2018**; 27(4): 378–385.
46. Danso MO, van Drongelen V, Mulder A, van Esch J, Scott H, van Smeden J, et al. TNF-A and Th2 cytokines induce atopic dermatitis–like features on epidermal differentiation proteins and stratum corneum lipids in human skin equivalents. **J Invest Dermatol 2014**; 134(7): 1941–1950.
47. Chen D, Oezguen N, Urvil P, Ferguson C, Dann SM, Savidge TC. Regulation of protein-ligand binding affinity by hydrogen bond pairing. **Sci Adv 2016**; 2(3):e1501240.
48. Meylani V, Rizal Putra R, Miftahussurur M, Sukardiman S, Hermanto FE, Abdullah A. Molecular docking analysis of Cinnamomum zeylanicum phytochemicals against secreted aspartyl proteinase 4-6 of Candida albicans as anti-candidiasis oral. **Results Chem 2023**; 5:100721.
49. van den Noort M, de Boer M, Poolman B. Stability of ligand-induced protein conformation influences affinity in maltose-binding protein. **J Mol Biol 2021**; 433(15):167036.

50. Celej MS, Montich GG, Fidelio GD. Protein stability induced by ligand binding correlates with changes in protein flexibility. **Protein Sci 2003**; 12(7): 1496–1506.
51. Wankowicz SA, de Oliveira SH, Hogan DW, van den Bedem H, Fraser JS. Ligand binding remodels protein side-chain conformational heterogeneity. In: Brunger AT, Dötsch V, editors. **eLife**, vol. 11; 2022, e74114.
52. Zhang R, Zhang H, Shao S, Shen Y, Xiao F, Sun J, et al. Compound traditional Chinese medicine dermatitis ointment ameliorates inflammatory responses and dysregulation of itch-related molecules in atopic dermatitis. **Chin Med 2022**; 17: 3.
53. Hidayat S, Yoshino K ichi, Tokunaga C, Hara K, Matsuo M, Yonezawa K. Inhibition of amino acid-mTOR signaling by a leucine derivative induces G1 arrest in Jurkat cells. **Biochem Biophys Res Commun 2003**; 301(2): 417–423.
54. Pålsson-McDermott EM, O'Neill LAJ. Targeting immunometabolism as an anti-inflammatory strategy. **Cell Res 2020**; 30(4): 300–314.
55. De Bruyn Carlier T, Badloe FMS, Ring J, Gutermuth J, Kortekaas Krohn I. Autoreactive T cells and their role in atopic dermatitis. **J Autoimmun 2021**; 120:102634.
56. Lee JK, Kim KB, Lee JD, Shin CY, Kwack SJ, Lee BM, et al. Risk assessment of drometrizole, a cosmetic ingredient used as an ultraviolet light absorber. **Toxicol Res 2019**; 35(2): 119–129.
57. Piquero-Casals J, Carrascosa JM, Morgado-Carrasco D, Narda M, Trullas C, Granger C, et al. The role of photoprotection in optimizing the treatment of atopic dermatitis. **Dermatol Ther (Heidelb) 2021**; 11(2): 315–325.

How to cite this article: Pandaleke TA, Handono K, Widasmara D, Susianti H. The immunomodulatory activity of *Orthosiphon aristatus* against atopic dermatitis: Evidence-based on network pharmacology and molecular simulations. J Taibah Univ Med Sc 2024;19(1):164–174.